Numerical Evaluation of Stress Intensity Factors of Three-dimensional Surface Cracks in Welded Joints Using the Superposition Method

by Ramy Gadallah*, *Student Member* Naoki Osawa*, *Member*
Satoyuki Tanaka**, *Member*

Key Words: *Superposition Method, Crack Face Traction, SIFs, Surface Crack, Residual Stress Field*

1. INTRODUCTION

Cracks are one of the main factors influencing the structural integrity of ships, offshore platforms, pressure vessels and other structures. Surface cracks occur frequently at weld toes [1]. These cracks take various shapes, for example, cracks in fillet welded joints show long-shallow shapes. For linear elastic fracture mechanics problems, the principle of superposition is effective for cracks in residual stress fields and crack cohesive force models. However in case of simple crack problems, they are usually analyzed by applying remote loads. For example, when analyzing a crack in a residual stress field, the influence of the stress field can be taken into account through applying a traction force on crack faces, where the value of traction force is the negative of the stress field [2].

It is important to examine the accuracy of numerical domain/interaction integration methods for crack face traction force cases. In this study, the principle of superposition is applied for 3D surface cracks in flat plate and T-butt welded models. This study shows the significance of the crack face traction term for obtaining accurate calculated stress intensity factors (SIFs).

2. THEORETICAL BACKGROUND

2.1 Principle of Superposition

The principle of superposition can be used to evaluate SIFs of a crack in a complex stress field, which may be resulted due to service loading and residual stress, by dividing the complex loading configuration into simple cases [1].

The principle of superposition cannot be used for adding SIFs (K values) of different loading mode conditions, i.e. modes I, II, and III [3]. In addition, it cannot be applied for models with different displacement boundary conditions. The principle can be only used for the same loading modes and the same displacement boundary conditions.

Figure 1 shows the principle of superposition of a semi-elliptical surface cracked body subjected to a uniform remote stress configuration. Based on the principle of superposition, the SIF ($K_I^{(a)}$) of the cracked body subjected to remote stress condition σ (Fig. 1(a)) is equal to that ($K_I^{(c)}$) of the cracked body subjected to crack face loading σ (Fig. 1(c)). The SIF ($K_I^{(b)}$) for the body loaded with the remote stress condition (σ) and the crack faces closing stress (– σ) in Fig. 1(b) equals zero, i.e. $K_I^{(b)} = 0$, because the crack faces are closed and the body behaves as if there is no crack under such conditions [3].

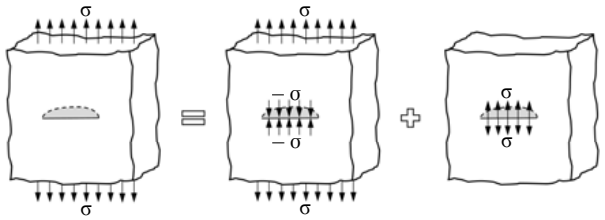

(a) (b) (c)

$$K_I^{(a)} = K_I^{(b)} + K_I^{(c)} = K_I^{(c)} \qquad (since\ K_I^{(b)} = 0)$$

Fig.1 Determination of SIF (K_I) for a semi-elliptical surface cracked body subject to a uniform remote stress using the principle of superposition.

2.2 The Domain Integral for 3D Cracks

The domain integral method was developed by Shih et al. [4] and it is considered as a powerful numerical method to calculate the J-integral for 3D cracks. The general formula of the J-integral requires that the contour surrounding the crack front be very small [3]. The J-integral at location s (see Fig. 2) along a 3D crack front has the general formula [4]:

$$J(s) = \lim_{\Gamma \to 0} \int_{\Gamma} (W\delta_{1i} - \sigma_{ij} u_{j,1}) n_i d\Gamma \qquad (1)$$

where W is strain energy density, δ_{ij} denotes the Kronecker delta, σ_{ij} is stress components, and u_j represents displacement components. The contour Γ, with normal vector components n_i, exists in X_1–X_2 plane in the local coordinate system, and it starts from the lower crack face and ends at the upper crack face as shown in Fig. 2.

Shih et al. [4] formulated Eq. (1) into two main parts: 1) volume integral, and 2) surface integral to be suitable for numerical analysis in case of 3D cracks. They formulated the energy released per unit advance of crack front segment L_C, $\overline{J}(s)$, as follows:

$$\overline{J}(s) = \int_V (\sigma_{ij} u_{j,1} - W\delta_{1i}) q_{,i} dV + \int_V (\sigma_{ij} u_{j,1} - W\delta_{1i})_{,i} q dV - \int_{S^+ + S^-} t_j u_{j,1} q dS \qquad (2)$$

* Graduate School of Engineering, Osaka University
** Graduate School of Engineering, Hiroshima University
Recieved 25th September 2015
Read at the autumn meeting 16th and 17th NOV. 2015

where t_j are crack face traction components. Surfaces S^+, S^-, S_1, S_t, S_2 and S_3 (see Fig. 2) form volume V, and surface S_t shrinks to the crack front (i.e. $r \rightarrow 0$). The weight function q, varies smoothly within volume V. Equation (2) requires that $q = 0$ at S_1, S_2, and S_3 and equals 1.0 at location s on S_t [4].

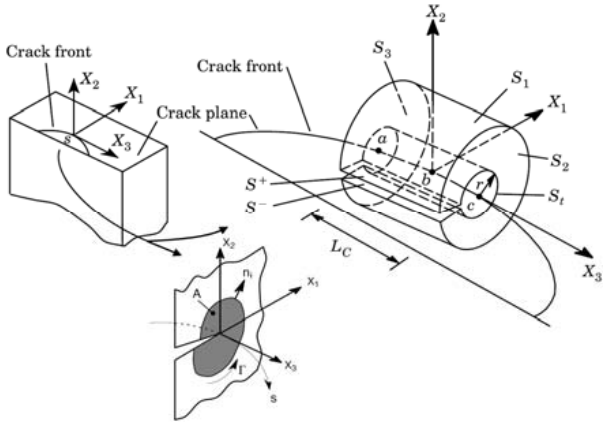

Fig.2 Finite volume for use in Domain Integral formulation at crack front location s which extends over length L_C [5].

The second and third integrals in Eq. (2) are vanished for elastic, homogenous materials under quasi-static, isothermal loading in case of body forces or crack face tractions are absent [5]. These two integrals (second and third integrals) are omitted in commercial nonlinear finite element (FE) codes (e.g. MSC Marc, Abaqus, ANSYS, etc.). Shih et al. [4] derived the approximate formula of the J-integral by assuming that the energy release rate varies slowly over L_C:

$$J(s) = \frac{\overline{J}(s)}{\int_{L_C} q(s)ds} \tag{3}$$

The SIFs for the three modes can be calculated using the J-integral, $J(s)$, in Eq. (3) as follows [6]:

$$K_I = \sqrt{J(s)E^*}\ , K_{II} = \sqrt{J(s)E^*}\ , \text{and}\ \ K_{III} = \sqrt{\frac{J(s)E}{(1+\nu)}} \tag{4}$$

where $E^* = E$ for plane stress condition and $E^* = E/(1 - \nu^2)$ for plane strain condition.

2.3 The Interaction Integral for 3D Cracks

The interaction integral method gives actual displacement, stress, and strain fields of an equilibrium state for a boundary value problem. In addition, auxiliary fields that include desired quantities such as SIFs or T-stresses can be provided by another selected equilibrium state [6]. By superimposing actual equilibrium fields with auxiliary fields, $\overline{J}(s)$ for the superimposed state, $\overline{J}^S$, from Eq. (2) becomes [5]:

$$\begin{aligned}\overline{J}^S(s) = &\int_V [(\sigma_{ij} + \sigma_{ij}^{aux})(u_{j,1} + u_{j,1}^{aux}) - W^S\delta_{1i}]q_{,i}dV + \\ &\int_V [(\sigma_{ij} + \sigma_{ij}^{aux})(u_{j,1} + u_{j,1}^{aux}) - W^S\delta_{1i}]_{,i}qdV - \\ &\int_{S^+ + S^-} (t_j + t_j^{aux})(u_{j,1} + u_{j,1}^{aux})qdS\end{aligned} \tag{5}$$

The superscript 'S' represents the superimposed state. For a linear-elastic material, the strain energy density for the superimposed state, W^S, is [5]:

$$W^S = \tfrac{1}{2}(\sigma_{ij} + \sigma_{ij}^{aux})(\varepsilon_{ij} + \varepsilon_{ij}^{aux}) = W + W^{aux} + W^I \tag{6}$$

With Eq. (6), $\overline{J}^S$ divides into three terms [5]:

$$\overline{J}^S(s) = \overline{J}(s) + \overline{J}^{aux}(s) + \overline{I}(s) \tag{7}$$

Where $\overline{J}(s)$ equals Eq. (2), the domain integral for the actual state; $\overline{J}^{aux}(s)$ is the domain integral for the auxiliary state; and $\overline{I}(s)$ is the domain for the interaction integral, defined as [5]:

$$\begin{aligned}\overline{I}(s) = &\int_V (\sigma_{ij}u_{j,1}^{aux} + \sigma_{ij}^{aux}u_{j,1} - \sigma_{jk}\varepsilon_{jk}^{aux}\delta_{1i})q_{,i}dV + \\ &\int_V [\sigma_{ij}(u_{j,1i}^{aux} - \varepsilon_{ij,1}^{aux}) + \sigma_{ij,1}^{aux}u_{j,1}]qdV - \int_{S^+ + S^-} t_j u_{j,1}^{aux}qdS\end{aligned} \tag{8}$$

The third term in Eq. (8), $\int_{S^+ + S^-} t_j u_{j,1}^{aux}qdS$, represents the crack face integral. This integral has a significant contribution to the accuracy of calculated SIFs. All the quantities in the crack face integral do not rely on the finite element solution of the boundary value problem [5].

By calculating the value of $\overline{I}(s)$ from Eq. (8), the interaction integral calculation at location s (see Fig. 2) over a 3D crack front follows Eq. (3) [5]:

$$I(s) = \frac{\overline{I}(s)}{\int_{L_C} q(s)ds} \tag{9}$$

After calculating $I(s)$ from Eq. (9), the SIFs for the three modes can be calculated as follows [5]:

$$K_I = \tfrac{E^*}{2}I(s)\ , K_{II} = \tfrac{E^*}{2}I(s)\ , \text{and}\ \ K_{III} = \mu I(s) \tag{10}$$

where $\mu = E/2(1+\nu)$, E^* conditions are defined previously in Eq. (4). For more details about the interaction integral method, refer to [5, 6].

3. NUMERICAL ANALYSES

3.1 Models Definition

In the present study, flat plate and T-butt welded joint with surface cracks are employed as shown in Fig. 3. The T-butt model, used in this study, is one-side welded model with radiused weld toe as used by Bowness and Lee [7]. Two cases per each model are investigated to examine the accuracy of the numerical solutions such as domain integral and interaction integral methods for crack face traction cases. The dimensions of crack, crack aspect ratios, and crack depth ratios for each case are shown in Table 1, where a is crack depth, c is crack half length, and t is model thickness.

The finite element models corresponding to Fig. 3 are shown in Fig. 4. The arrows in Fig. 4 show the applied boundary conditions. For the sake of simplicity, few arrows are used to show the symmetry around the longitudinal axis. The FE mesh on the crack face for the flat plate and T-butt welded models are shown in Fig. 5. The flat plate models are generated using FEAcrack software [8]. The T-butt welded models are generated in two steps: 1) create crack block using

Zencrack software [9], and 2) generate the global model that consists of flat plate with attachment using Patran software. The crack block is tied to the global model using glue contact. For the T-butt welded model, a FORTRAN program is developed to automatically create the radiused welded toe.

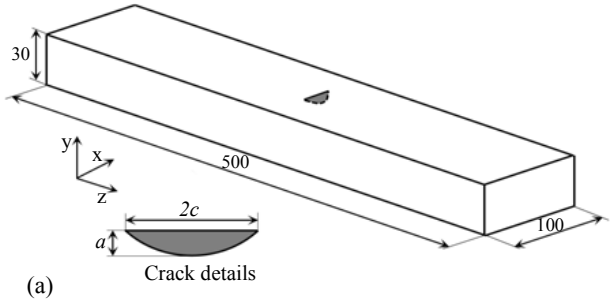

(a)

All dimensions in mm.

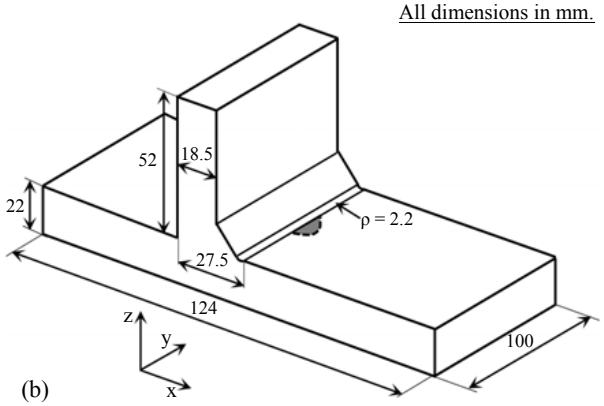

(b)

Fig.3 Surface cracked bodies. (a) flat plate, and (b) T-butt welded joint (where ρ is the radius of weld toe).

Table1 Crack dimensions (*a* and *c*), crack aspect ratios (*a*/*c*), and crack depth ratios (*a*/*t*) for flat plate and T-butt welded models.

Model	Case	*a*	*c*	*a*/*c*	*a*/*t*
Flat plate	case 1	3.6	6.1	0.59	0.12
	case 2	5.8	12.6	0.46	0.19
T-butt joint	case 1	4.0	4.0	1.00	0.18
	case 2	3.3	4.7	0.70	0.15

Finite element mesh of the cracked models are generated using 20-noded isoparametric hexahedral brick elements. Along the crack front, the 20-noded hexahedral elements are collapsed to quarter-point wedge elements which used to simulate the $1/\sqrt{r}$ singularity of the stress field close to the crack front. The Young's modulus and Poisson's ratio used in the analyses are 210 GPa and 0.3, respectively. Since the models are symmetric around the longitudinal axis, half-models are used in the analyses. The rigid body motion of the models are prevented by applying the minimum displacement constraints.

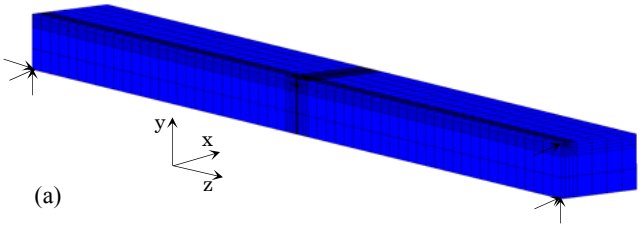

(a)

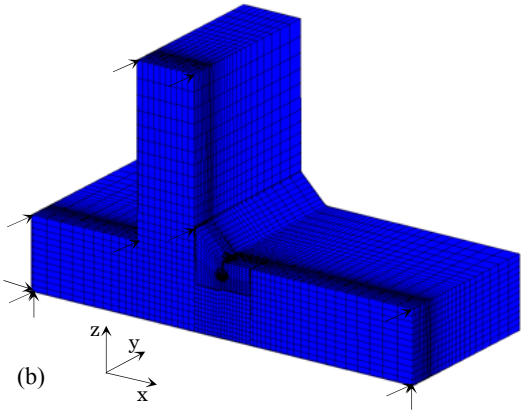

(b)

Fig.4 Finite element half-model with boundary conditions for (a) flat plate, and (b) T-butt welded joint.

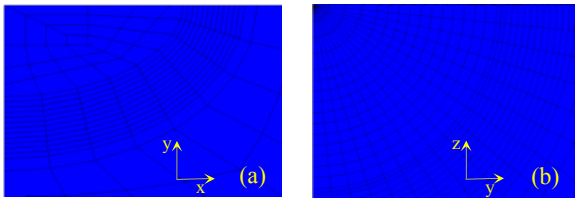

Fig.5 The FE mesh on the crack face. (a) flat plate, and (b) T-butt welded joint.

In this study, linear elastic fracture mechanics approach is performed. The cracked models (flat plate and T-butt joint) are subject to uniaxial uniform remote tensile loading in the longitudinal direction. In the current study, the superposition method is implemented in three steps (see Fig. 1): 1) calculation of K_I values by applying uniform remote tensile loading for the cracked flat plate and cracked T-butt welded models (i.e. direct solution), 2) residual stress filed at the crack plane is calculated by applying the same remote tensile loading for geometrically identical uncracked models, and 3) K_I values are calculated using the stress field which applied for geometrically identical cracked models. To examine the effectiveness of the crack face traction term on the calculated SIFs using crack face tractions, this study is divided into two parts: 1) calculation of SIFs using face tractions without considering the crack face traction term, and 2) calculation of SIFs using face tractions with considering the crack face traction term.

3.2 Calculation of SIFs Using Face Tractions without Considering the Crack Face Traction Term

In this section, the SIFs are evaluated using the superposition method without considering the crack face traction term for surface cracks in flat plate and T-butt welded models. The fracture mechanics parameters (SIFs) are evaluated based on the domain integral method employing the crack option of MSC Marc. As mentioned previously, MSC Marc solver does not provide the crack face traction integral in the domain integral solution. The validity of the calculated SIFs (K_I values) by remote tensile loading for the cases of flat plate model are examined by the solution of Newman-Raju [10]. For the T-butt welded model, the SIFs calculated by remote tensile loading are validated with those computed by Tanaka et al. [11]. The same displacement boundary conditions are used for the three steps of the superposition method those

mentioned in section 3.1 and shown Fig. 4.

(1) Flat Plate Model

As it is well known, for simple geometries such as flat plate, the remote tensile loading that applied for uncracked flat plate model arises uniform distributed residual stress field at the crack plane. To reduce the man-hour needed to prepare the crack nodal forces from the produced residual stress field, a FORTRAN program is developed to handle the generated stress field. The handled residual stress field is used as nodal forces (i.e. crack nodal tractions) at the crack face nodes for the cracked model with opposite sign in order to calculate the stress intensity factor (K_I) values owing to the induced stress field. The crack nodal tractions try to open the crack as in the case of remote tensile loading (see Fig. 1). The accuracy of the numerical domain integral method for crack nodal traction cases is examined by comparing the calculated SIFs (K_I values) using the crack nodal tractions with those calculated by the remote tensile loading. To validate the solutions, i.e. calculated SIFs by direct solution and crack nodal tractions, the total strain energy (U) and the crack mouth opening displacement (CMOD) for the solutions are examined as shown in Table 2. For the sake of simplicity, the results of U and CMOD for case 1 are only shown in Table 2.

Figure 6 shows the distribution of the non-dimensional SIFs (mode-I) calculated by remote load and crack nodal tractions for case 1 and case 2. It is clear that there is difference between the SIFs calculated by the two solutions (i.e. direct solution and crack nodal tractions). The difference between the two solutions is due to the absence of the crack face traction term in the domain integral solution, the crack face traction integral in the current solution is omitted from Eq. (2). The difference percent between the SIF (K_I value) calculated by the direct solution and that calculated by the crack nodal tractions at the deepest point of the crack (at $2\varphi/\pi = 1$) is 4.4% for case 1 and 4.6% for case 2.

Table2 Validation of the solutions using total strain energy (U) and CMOD for flat plate model (case 1). The results based on Fig. 1. [Note that: w_1 and w_2 are longitudinal displacements].

$U_{(a)}$	$U_{(b)}$	$U_{(c)}$	$U_{(b)} + U_{(c)}$	Difference between $U_{(a)}$ & $U_{(b)} + U_{(c)}$
1.79E+00	1.79E+00	3.33E-04	1.79E+00	0.000409619%
Case	w_1	w_2	CMOD	Difference between $CMOD_{(a)}$ & $CMOD_{(c)}$
Fig. 1(a)	1.16E-03	1.22E-03	6.74E-05	0.002671344%
Fig. 1(c)	-3.41E-05	3.33E-05	6.74E-05	

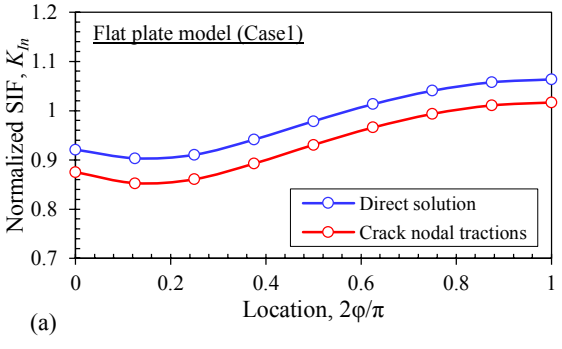

(a)

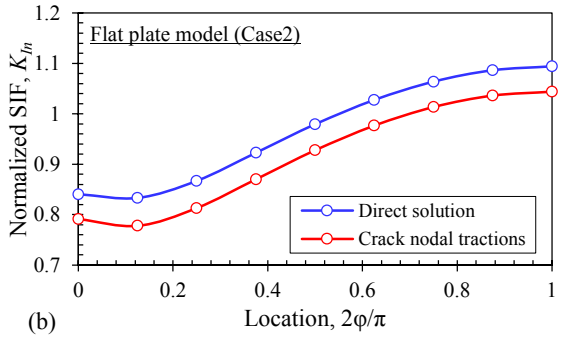

(b)

Fig.6 Distribution of the SIFs (mode-I) calculated by direct solution and crack nodal tractions for the flat plate model in case of crack face traction term is not considered. (a) case 1, and (b) case 2.

(2) T-butt Welded Model

In case of the T-butt welded model, glue contact option is employed using MSC Marc in order to tie the crack block with the global model. The applied glue contact in the current analyses does not have significant influence on the calculated SIFs. For the T-butt welded model, due to the stress concentration at the weld toe, a non-uniform residual stress field is introduced at the crack plane when remote tensile loading is applied for uncracked model. The SIFs using crack nodal tractions are calculated by following the same procedures those explained in the case of flat plate model. In the same way, Table 3 shows the validity of the solutions using the total strain energy and the CMOD for case 1 only.

Figure 7 shows the distribution of the non-dimensional SIFs (mode-I) calculated by direct solution and crack nodal tractions for case 1 and case 2. Again as in the case of flat plate model, a difference between the direct solution and crack nodal traction solution is observed for the two cases for the same reason. The difference percent between the SIF (K_I value) calculated by the crack nodal tractions and that calculated by the direct solution at the deepest point of the crack (at $2\varphi/\pi = 1$) is 4.3% for case 1 and 4.8% for case 2.

Table3 Validation of the solutions using total strain energy (U) and CMOD for T-butt welded model (case 1). The results based on Fig. 1. [Note that: u_1 and u_2 are longitudinal displacements].

$U_{(a)}$	$U_{(b)}$	$U_{(c)}$	$U_{(b)} + U_{(c)}$	Difference between $U_{(a)}$ & $U_{(b)} + U_{(c)}$
1.28E+04	1.28E+04	1.03E+01	1.28E+04	0.004870917%
Case	u_1	u_2	CMOD	Difference between $CMOD_{(a)}$ & $CMOD_{(c)}$
Fig. 1(a)	5.28E-02	6.43E-02	1.15E-02	0.275695326%
Fig. 1(c)	-4.91E-03	6.55E-03	1.15E-02	

(3) Discussion

As shown in Tables 2 and 3, the difference between the total strain energies (i.e. $U_{(a)}$ and $U_{(b)} + U_{(c)}$) and the difference between the crack mouth opening displacements (i.e. $CMOD_{(a)}$ and $CMOD_{(c)}$) for the solutions are negligible. On the other hand, it is known that the crack face traction term is needed when considering surface tractions in the domain integral method [1, 5]. Although the crack face traction term is not considered in the domain integral of MSC Marc, the results of the numerical analyses for the flat plate and T-butt welded

models show good accuracy for the domain integral. It is found that the difference between the solutions (i.e. direct solution and crack nodal tractions) for both the flat plate and T-butt welded models at the deepest point of the crack is less than 5% even if the surface traction force term in the domain integral solution is neglected. This shows that the superposition method can be applied for engineering problems using commercial nonlinear FE codes under the conditions chosen in the present study.

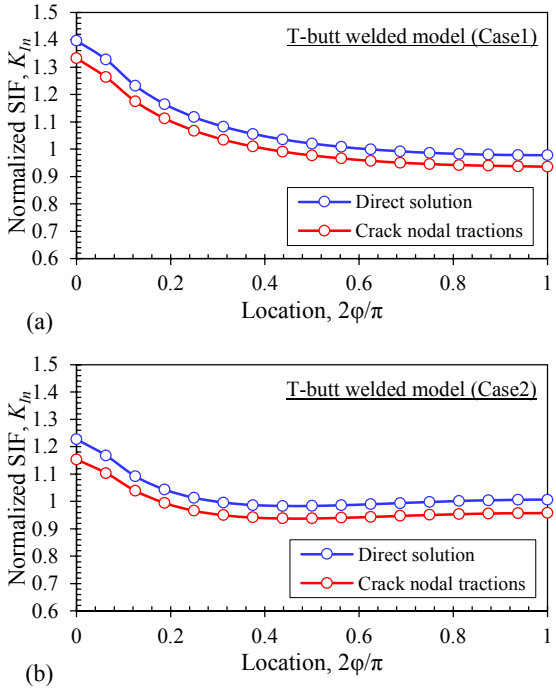

Fig.7 Distribution of the SIFs (mode-I) calculated by direct solution and crack nodal tractions for the T-butt welded model in case of crack face traction term is not considered. (a) case 1, and (b) case 2.

3.3 Calculation of SIFs Using Face Tractions with Considering the Crack Face Traction Term

In this part, the SIFs are evaluated using the superposition method considering the crack face traction term for surface cracks in the flat plate models only. The interaction integral method is used to evaluate the SIFs using the WARP3D code [6]. WARP3D is an open source research code for nonlinear finite element analysis (FEA) of large-scale, 3D solids and structures subjected to static and dynamic loads. The crack face traction term is implemented in the interaction integral method for a uniform distributed residual stress field only. Thus, in this section, the numerical analyses are performed only for the flat plate model. The two cases of the flat plate model those used in section 3.2 are also employed in this section with the same displacement boundary conditions and the same remote tensile loading configuration.

The validity of the SIFs (K_I values) calculated by the interaction integral using remote tensile loading is examined by the solution of Newman-Raju [10]. Since the produced residual stress field at the crack plane for the uncracked model is uniform, the applied remote loading is used directly with inverse sign as a traction pressure on the crack faces. The effectiveness of the crack face traction term in the interaction integral method is examined by comparing the numerical results (i.e. SIFs) computed by direct solution and those computed by crack face tractions. Table 4 shows the validation of the solutions using the CMOD for case 1 only. It is clear that the difference between $CMOD_{(a)}$ and $CMOD_{(c)}$ is negligible.

Figure 8 shows the distribution of the non-dimensional SIFs (mode-I) calculated by direct solution and crack face tractions for case 1 and case 2. From Fig. 8, excellent agreement (except at the crack end at $2\varphi/\pi = 0$) between the two solutions is obtained. For example, the difference percent at the deepest point of the crack (at $2\varphi/\pi = 1$) between the SIF (K_I value) calculated by the crack face traction and that calculated by direct solution is 0.39% for case 1 and 0.28% for case 2.

Table4 Validation of the solutions using the CMOD for flat plate model (case 1). The results based on Fig. 1. [Note that: w_1 and w_2 are longitudinal displacements].

Case	w_1	w_2	CMOD	Difference between $CMOD_{(a)}$ & $CMOD_{(c)}$
Fig. 1(a)	1.16E-03	1.22E-03	6.75E-05	0.017777778%
Fig. 1(c)	-3.41E-05	3.34E-05	6.75E-05	

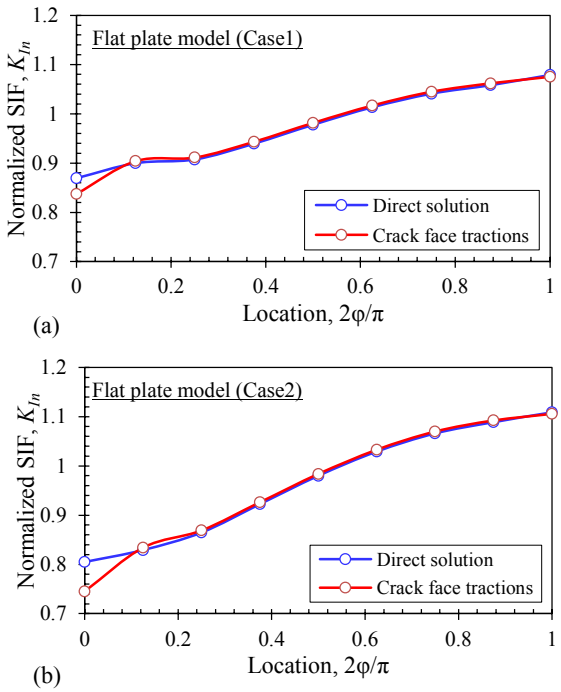

Fig.8 Distribution of the SIFs (mode-I) calculated by direct solution and crack face tractions for the flat plate model in case of crack face traction term is considered. (a) case 1, and (b) case 2.

To clearly show the effectiveness of the crack face traction term on the accuracy of the SIFs computed by crack face tractions, the computed SIFs with and without considering the crack face traction term are compared together; as shown in Fig. 9. The direct solutions using remote loading system those obtained by the domain integral and the interaction integral methods are used in Fig. 9 as references for the purpose of comparison. It is observed that the crack face traction term significantly improves the solution of the calculated SIFs using surface tractions. The crack face traction term increases the

accuracy of the calculated SIFs using crack face tractions by 5–6.5% for both case 1 and case 2.

For future work, in order to implement the crack face traction term for a T-butt welded joint subjected to remote tensile loading and for a flat plate and a T-butt welded joint subjected to bending loading (i.e. non-uniform residual stress field at crack plane), the current code of the interaction integral method in the WARP3D should be modified.

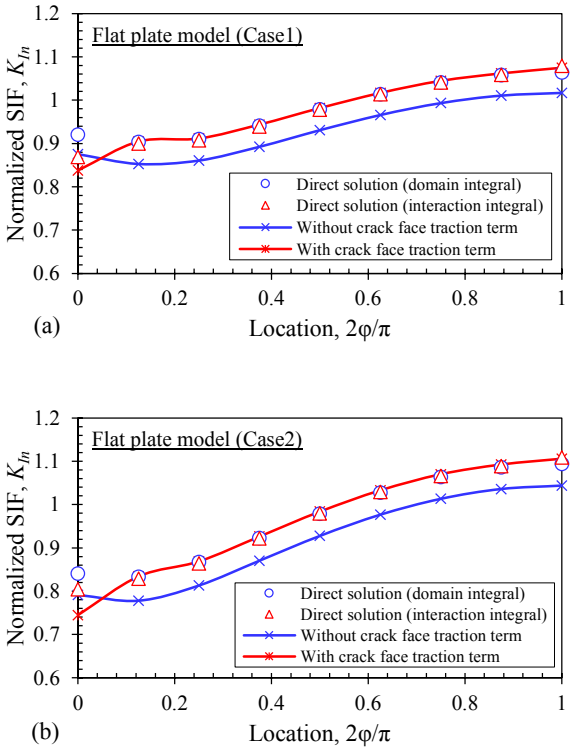

Fig.9 Comparison of the normalized SIFs (mode-I) calculated by direct solution and crack face tractions for the flat plate model. (a) case 1, and (b) case 2.

4. CONCLUDING REMARKS

In the present study, the superposition method is employed for 3D surface cracks in flat plate and T-butt welded models. The accuracy of the numerical domain and interaction integral methods for crack face traction cases is examined. This study is divided into two parts: 1) calculation of SIFs using face tractions without considering the crack face traction term, and 2) calculation of SIFs using face tractions with considering the crack face traction term. Based on the numerical analyses results, the following conclusions can be drawn:

1) Although the crack face traction term is neglected in the domain integral solution, a difference less than 5% at the deepest point of the crack between the solutions is obtained for the flat plate and T-butt welded models.
2) Commercial nonlinear FE codes those neglect the crack face traction term can be used for the engineering fracture mechanics problems under the conditions chosen in this study.
3) The effectiveness of the crack face traction term in the interaction integral method is demonstrated for the flat plate model. It is found that the difference between the solutions is less than 0.5% at the deepest point of the crack.
4) The crack face traction term clearly improves the calculated SIFs using crack face tractions by 5–6.5% for the flat plate model.

REFERENCES

1) Y. Lu: A practical procedure for evaluating SIFs along fronts of semi-elliptical surface cracks at weld toes in complex stress fields, Int. J. Fatigue, Vol. 18, No. 2, pp.127–135, 1996.
2) T. Nagashima and N. Miura: Crack analysis in residual stress field by X-FEM, J. Comp. Sci. & Tech., Vol. 3, No. 1, pp.136–147, 2009.
3) T.L. Anderson: Fracture mechanics: fundamentals and applications, 3rd ed., CRC Press, 2005.
4) C.F. Shih, B. Moran, and T. Nakamura: Energy release rate along a three-dimensional crack front in a thermally stressed body, Int. J. Fract., Vol.30, pp.79–102, 1986.
5) M.C. Walters, G.H. Paulino, and R.H. Dodds: Interaction integral procedures for 3-D curved cracks including surface tractions, Eng. Fract. Mech., Vol. 72, pp.1635–1663, 2005.
6) B. Healy *et al.:* WARP3D–release 17.6.0 manual, Report No. UILU-ENG-95-2012, Civil Engineering, University of Illinois, Urbana, IL 61801, USA, 2015.
7) D. Bowness and M.M.K. Lee: Prediction of weld toe magnification factors for semi-elliptical cracks in T-butt joints, Int. J. Fatigue, Vol. 22, pp.369–387, 2000.
8) Quest integrity group, FEAcrack FEACrack 3D finite element software for cracks, Version 3.2, User's manual, 2010.
9) Zentech Inc., ZENCRACK 7.2, User's manual, 2003.
10) J.C. Newman and I.S. Raju: Stress-intensity factor equations for cracks in three-dimensional finite bodies subjected to tension and bending loads, NASA technical memorandum, NASA TM-85793, 1984.
11) S. Tanaka, T. Kawahara, and H. Okada: Study on crack propagation simulation of surface crack in welded joint structure, Marine Struct., Vol. 39, pp.315–334, 2014.